Characterization and Thermal Treatment of Carbon-14 on Irradiated Graphite Surfaces III– 14204

Mary Lou Dunzik-Gougar
James Cleaver, Daniel LaBrier, Shilo McCrory, Kathy Nelson and Tara E. Smith
Idaho State University: 1776 Science Center Dr., Idaho Falls, ID, 83401

ABSTRACT

The aim of the research presented at WM12 and updated at WM13 and this year is to identify the chemical form of C-14 in irradiated graphite. A greater understanding of the chemical form of this longest-lived isotope in irradiated graphite will inform not only management of legacy waste, but also development of next generation gas-cooled reactors. Approximately 250,000 metric tons of irradiated graphite waste exists worldwide, with the largest single quantity originating in the Magnox and AGR reactors of UK. The waste quantity is expected to increase with decommissioning of Generation II reactors and deployment of Generation IV gas-cooled, graphite moderated reactors. Of greatest concern for long-term disposal of irradiated graphite is carbon-14 (C-14), with a half-life of 5730 years.

Study of irradiated graphite from some nuclear reactors indicates a C-14 concentration in the outer 5 mm of the graphite structure. Characterization of irradiated graphite surfaces has been performed in parallel with treatment of the same material for removal of the labile C-14. Results of each process inform the other.

A nuclear-grade graphite, NBG-18, and a high-surface-area graphite foam, POCOFoam, were exposed to liquid nitrogen (to increase the quantity of C-14 precursor) and neutron-irradiated (10^{13} neutrons/cm^2/s). Finer grained NBG-25 was not exposed to liquid nitrogen prior to irradiation at a neutron flux on the order of 10^{14} /cm^2/s. Characterization of pre- and post-irradiation graphite was conducted to determine the chemical environment and quantity of C-14 and its precursors via the use of surface sensitive characterization techniques. The concentration, chemical composition, and bonding characteristics of C-14 and its precursors were determined through X-ray Photoelectron Spectroscopy (XPS), Time-of-Flight Secondary Ion Mass Spectrometry (SIMS), and Energy Dispersive X-ray Analysis Spectroscopy (EDX). Results of post-irradiation characterization of these materials indicate a variety of surface functional groups containing carbon, oxygen, nitrogen and hydrogen. Specifically, aldehydes, carboxylics, lactones, ethers, ketones and quinones are indicated. Further, results of post-thermal treatment characterization suggest graphite surfaces are returned to pre-irradiation composition, if not structure.

During thermal treatment, irradiated graphite samples are heated in the presence of an inert carrier gas (with or without oxidant gas), which carries off gaseous products released during treatment. Graphite gasification occurs via interaction with adsorbed oxygen complexes. Lower temperatures and oxygen levels correlated to more efficient C-14 removal. Based on these results, pre-treatment loading of oxygen to the surface is being pursued.

INTRODUCTION

Throughout the word during the past 50 years graphite has been widely used as a moderator, reflector, and fuel matrix in a variety of gas-cooled reactors. The result is approximately 250,000 metric tons of irradiated graphite waste [1]. Currently, the U.S. and other countries are developing High Temperature Gas-cooled Reactors (HTGR) using helium coolant, graphite-coated fuel particles, a graphite reflector, and other graphite core structural components [2]. These next generation HTGRs would dramatically add to the present quantity of irradiated graphite waste.

Characterization of existing irradiated graphite indicates that the most significant long-lived radioisotope is carbon-14 (C-14). With a half-life of 5,730 years this species is of concern for deep geologic disposal of irradiated graphite because it is readily mobile in groundwater and atmospheric systems [3]. Removal of C-14 from large irradiated graphite reactor components may reduce disposal cost, while also allowing the possibility of recycling

this very pure nuclear grade material [4]. However, to optimize the removal of C-14, it is important to understand the bonding characteristics, functional groups, location, and concentration of C-14.

Formation of C-14

While C-14 is produced by several routes (Eqn. 1 – 3) during neutron irradiation of graphite, the reaction of most significance for the surface, labile C-14 component is that involving N-14 [3].

N-14 +*n* -> C-14 +*p* (Eqn. 1)
C-13 +*n*-> C-14 + *gamma* (Eqn. 2)
O-17 +*n* -> C-14 + *alpha* (Eqn. 3)

Characterization of graphite from reactors, and of graphite irradiated for this study, reveals a significant C-14 concentration gradient from the surfaces to micrometers below [5,6]. Because O-17 is present at very low concentrations and C-13 is homogeneously distributed throughout graphite, it is most likely the C-14 surface concentration originates with N-14 on graphite surfaces and open porosity [5]. (See Table I)

Table I. Properties of C-14 Precursors

Species	Capture Cross Section (Barns)	Isotopic Abundance (%)
N-14	1.8	99.63 (N-14:N)
C-13	0.0015	1.07 (C-13:C)
O-17	0.235	0.04 (O-17:O)

Characterization

Production of C-14 significantly depends on the amount of nitrogen present. Directly analyzing graphite for C-14 is difficult because it is chemically indistinguishable from C-12. Furthermore, the difference in mass between N-14 and C-14 is only 0.001385 amu, rendering mass spectrometry based techniques ineffective in discriminating between the two. Therefore, preliminary characterization emphasized the N-14 pathway to formation of C-14 and the resulting environment in irradiated graphite [7].

The localization of C-14 on the surface of the graphite dictates the use of surface sensitive characterization techniques, though no single technique provides a complete understanding of the morphological features, chemical environment, location, and bonding characteristics. Scanning Electron Microscopy (SEM), X-Ray Diffraction (XRD), and Raman Spectroscopy (Raman) were used to evaluate the graphite's morphological features. The concentration, chemical composition, and bonding characteristics were determined through X-ray Photoelectron Spectroscopy (XPS), Secondary Ion Mass Spectrometry (SIMS), and Energy Dispersive X-ray Analysis (EDX).

Thermal Treatment

When graphite is heated at a constant temperature under forced convection with an inert gas it oxidizes due to the presence of adsorbed oxygen species, thus releasing gasified carbon-oxygen compounds (primarily as carbon monoxide) [8,9]. An oxidizing species also can be added to the carrier gas. If optimized, this process could be a viable strategy for graphite waste management given that the C-14 enriched surface oxidizes first. Further, the nature of off-gas species informs the characterization process.

Graphite oxidation rate is controlled by 3 mechanisms determined largely by the reaction temperature. At lower temperatures (less than about 600°C), oxidation kinetics is controlled by the chemical rate of reaction and at higher temperatures (above about 900°C) kinetics is dominated by diffusion of reactants and products through the product boundary layer. At intermediate temperatures, oxidation rate is controlled by diffusion of reactants and

products through graphite porosity. The temperatures of transition between oxidation kinetic regimes are highly dependent on the particular graphite properties and experimental conditions. The estimated transition temperatures are displayed in Table II [8,10,11]. The optimal temperature, and oxidation regime, for maximum C-14 removal will be specific to each graphite, but some general parameters can be established through experiments such as those reported here.

Table II. Expected Graphite Oxidation Kinetics Regime Temperature Boundaries

Regime 1 (C)	Regime 2 (C)	Regime 3 (C)
<(500-700)	> (500-700), < 900	900

METHOD

Unirradiated, irradiated and thermally treated irradiated samples of nuclear-grade graphites NBG-18 and NBG-25 (German-produced medium-grain and fine-grain graphite, respectively) and POCOFoam, a highly porous graphite foam, have been analyzed. The non-nuclear grade foam was chosen for its significant surface area [13]. NBG-18 and POCOFoam samples were immersed in liquid nitrogen (LN) for 24 hours prior to neutron irradiation. The purpose of LN immersion was to promote nitrogen adsorption and subsequent neutron-induced production of C-14 to ensure measurable quantities on sample surfaces. Typical C-14 concentrations in existing irradiated reactor graphite are on the order of parts-per-billion, which is too low for meaningful characterization. Sample irradiation took place at the MURR research reactor at the University of Missouri for 120 days in a thermal neutron flux of 6.7×10^{13} neutrons/cm^2/s. NBG-25 was not immersed in liquid nitrogen prior to irradiation at the Advanced Test Reactor (ATR) at Idaho National Laboratory for approximately 400 days at an average flux of 3×10^{14} neutrons/cm^2/s.

Graphite sample irradiation conditions for this project are summarized in Table III.

Table III. Graphite Irradiation

Graphite	Pre-irradiation Liquid N_2 Exposure	Facility	Time (days)	Flux (n/cm^2/s)
NBG-18	yes	MURR	120	10^{13} - 10^{14}
POCOFoam				
NBG-25	no	ATR	~400	3×10^{14}

Characterization

The surface sensitive techniques, SEM, XRD, Raman, EDX, XPS, and SIMS, were employed to characterize carbon bonding with nitrogen, oxygen, hydrogen and other carbons. Each technique was chosen to investigate a different aspect of the chemical nature of C-14.

Analysis was performed on NBG-18 & POCOFoam samples at each of the four stages of C-14 production: Unirradiated (non-LN immersed), LN immersed, irradiated, and thermally treated. Unirradiated, irradiated, and thermally treated NBG-25 samples also were analyzed.

XRD and Raman analyses of NBG-18 AND POCOFoam were discussed in the 2012 WMS publication [14]. Results of the SEM/EDX, XPS and SIMS analyses for all three graphite types were discussed in the 2013 WMS publication [15], focusing on differences in irradiated samples. In this paper, results of SEM/EDX, XPS, and SIMS analyses for irradiated and thermally treated irradiated samples of all three graphite types are presented.

SEM was used to identify the polycrystalline nature of the graphite. The implementation of SEM allows the texture, chemical composition, crystalline structure, and subsequently the orientation of the graphite to be viewed on sub-micron scales. The morphological features associated with the elemental and spatial chemical compositions were identified using EDX. NBG-18 and POCOFoam samples were polished in preparation for SEM/EDX analyses; NBG-25 samples were not polished. Surface areas that exhibited contrasting variations in elemental composition were targeted to map preferential nitrogen formation locations. These formation locations are denoted by color changes on the surface image after using visual graphing software. The compositional variations were measured with a 30 keV accelerating voltage and a 10 mm working distance on an EDX Genesis Quanta 3D FEG.

XPS was used to identify the concentration of surface species and specific carbon bonding types that eject core electrons of varying binding energies from the surface atoms. Binding energies are characteristic for each atom, and are direct representations of the atomic orbital energies [10]. Thus, the energy shifts associated with the movement of the elemental peak in the XPS spectrum are associated with changes in the chemical environment of the atoms. These variations lead to changes in the binding energies of the core electrons and can be used to further indicate the bonding structure of the atom. Graphite samples were studied via XPS using a VersaProbe PHI 5000 spectrometer with aluminum Kα radiation (1480.6 eV) and a base pressure of 2.6×10^{-5} Pa. The deconvoluted nitrogen (N 1s) and carbon (C 1s) peaks were used to determine the relative bonding configurations of the elements within the graphite. The peak shapes were filtered to yield a full-width-half-mass (FWHM) of 1.0 eV and as near a Gaussian fit as possible; however, the best fits of the C 1s and N 1s resulted in multiple Gaussian peaks. To ensure accuracy the energy scale was calibrated to reproduce the binding energies of Cu $2p_{3/2}$ (932.65 eV) and Au $4f_{7/2}$ (84.00 eV) and the sample charging was corrected by aligning the C 1s peak to 284.6 eV. The core level spectra were fitted using least squares in AugerScan 3.0 graphing software. Changes in the atomic concentrations, bonding configurations, and electronic structures of the target species were observed with respect to depth while sputtering the samples at a rate of 0.025 nm/sec.

SIMS was used to identify the carbon bonding configurations (with N, O, H and C) and the potential chemical environment by measuring displaced charged atomic and/or molecular species with a mass spectrometer. Graphite samples were analyzed via SIMS (TRIFT I spectrometer by PHI-EVANS). During analysis, samples were kept in a constant ultra-high vacuum environment of 7.3×10^{-11} Pa to reduce contamination in the chamber. The focused primary ion beam was rastered over an area of (50 x 50) μm^2 on the sample surface. Secondary ions were measured from a smaller region 20 μm^2 located at the center of the sputtered area. The accelerating voltage was set to 15.03 keV in the primary gallium ion source, and -3 keV on the sample surface resulting in a net voltage of 12.03 keV. Sputtering at a rate of 0.022 nm/sec allowed for variations in carbon-containing functional groups to be measured with respect to depth. Data was analyzed using WinCadence Version 3.41.

Thermal Treatment

Thermal treatment experiments performed to date are summarized in Table IV.

Table IV. Thermal Treatment Experimental Parameters

Gas Mixture		**Argon**			**Argon + 3 vol% O_2**		**Argon + 5 vol% O_2**	
	Temperature	**700°C**	**900°C**	**1400°C**	**700°C**	**1400°C**	**700°C**	**1400°C**
Graphite		**Experimental Run Time (hrs)***						
POCOFoam	Unirradiated	-	12,12	12,12,12	10,10,10	12,10,10	10,10,10	4,4,4
	Irradiated	-	12,10,10	10,10,10	10,10,7	1,1,1	7,7,7	1,1,1
NBG-18	Unirradiated	13,10	-	-	-	-	10,10	2,2
	Irradiated	13,13, 8, 8	-	-	-	-	10,10, 8, 8	2.5,2
NBG-25	Unirradiated	13	-	-	-	-	-	-
	Irradiated	13, 13, 8, 8	-	-	-	-	-	-

*Each run time represents a separate experiment.

In each experiment a pre-weighed graphite sample was placed in the center of the main furnace (Fig. 1). Experimental temperatures (700°C, 900°C and 1400°C) were chosen with the intent of facilitating oxidation in two different oxidation kinetic regimes. Argon carrier gas was flowed through the furnace to transport gasified oxidation products released from the graphite through the system to a collection bottle. In some experiments, the carrier gas was doped with 3 vol% (1.5 sccm) or 5 vol% (2.6 sccm) oxygen gas to increase the amount of graphite oxidation.

A small portion of gas leaving the furnace was diverted to a Hiden quadrupole mass spectrometer gas analyzer before returning to the main gas flow path. The gas analyzer was programmed to monitor for CO, CO_2, Ar, O_2, N_2, H_2O, CH_4, ^{14}CO, and $^{14}CO_2$. After this analysis all gas flowed through the 800°C oxidizing furnace where any C-containing species oxidized to CO_2 via reaction with granular copper oxide wrapped in copper mesh. This step ensured all C was converted to CO_2 for collection in a 4 M NaOH solution. Upon completion of an experiment the graphite was reweighed to determine the overall mass loss.

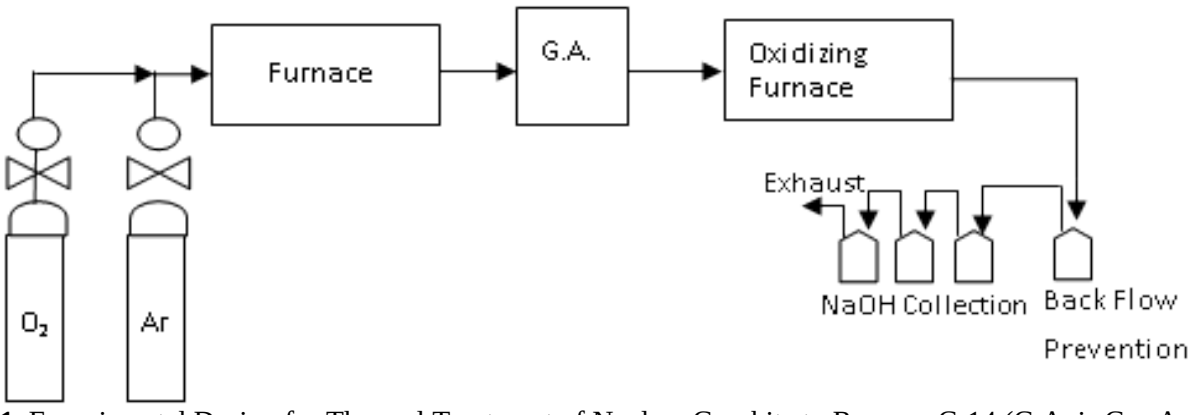

Fig. 1. Experimental Design for Thermal Treatment of Nuclear Graphite to Remove C-14 (G.A. is Gas Analyzer).

During experiments with irradiated graphite, gas collection bottles were sampled with respect to time and analyzed via liquid scintillation counting (LSC) to determine C-14 content and the associated rate of release from the graphite. Upon completion of irradiated thermal treatment experiments the reweighed sample was fully oxidized to determine the total C-14 content in the sample.

RESULTS

Characterization

Irradiated Graphite

SEM identified the formation of clusters in irradiated LN-immersed samples averaging in size from 5 to 10 μm attached to the surface and graphite planes; these clusters were not observed on the surface of irradiated NBG-25 (Fig. 2, all three graphite types). The surface composition of the clusters was further explored using EDX. The images displayed in Figs. 3 (POCOFoam) and 4 (NBG-18) show the location and qualitative concentrations of carbon (red), oxygen (blue), and nitrogen (green) atoms on the irradiated graphite surfaces. The EDX images illustrate that the clusters are preferentially located along plane edges and mainly composed of nitrogen.

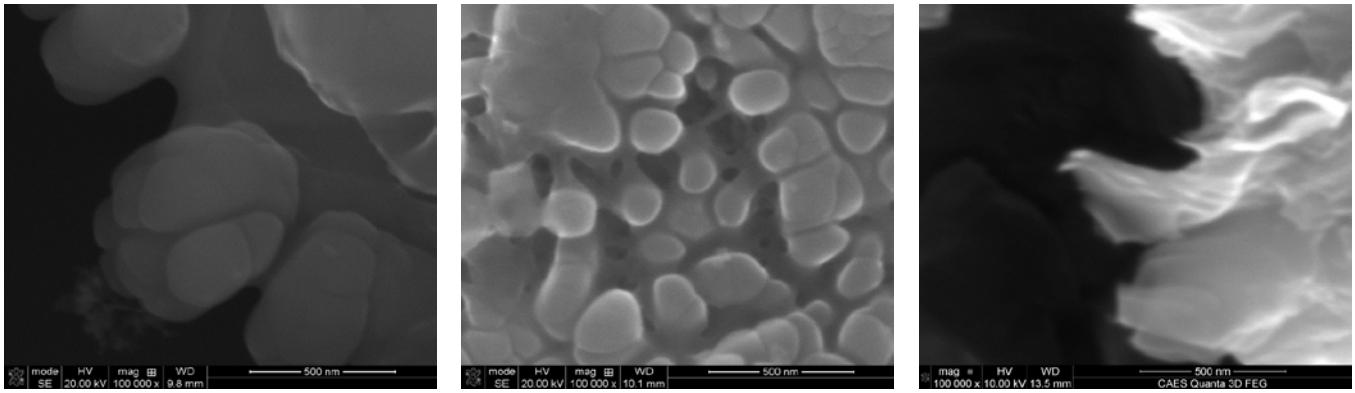

Fig. 2. SEM Images of irradiated POCOFoam (Left), NBG-18 (Center) and NBG-25 (Right) at 100,000x. Nitrogen clusters are observed on the graphite planar edges of POCOFoam and NBG-18 only.

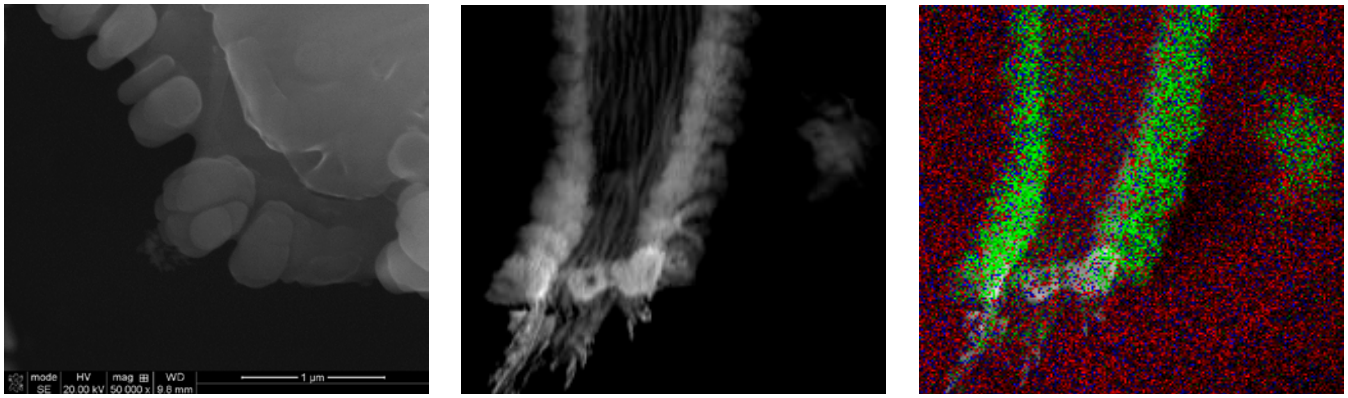

Fig. 3. SEM Image of irradiated POCOFoam at 50,000x (Left), and 5000x (Center); EDX image (Right) of Irradiated POCOFoam at 5,000x. All images show the presence of nitrogen clusters along graphite plane edges.

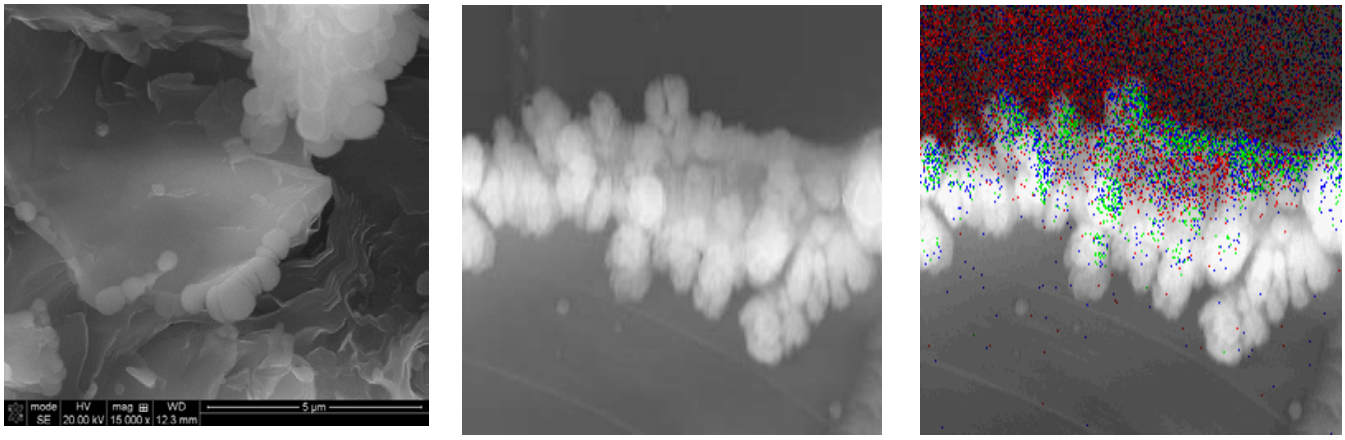

Fig. 4. SEM Image of irradiated NBG-18 at 15,000x (Left); SEM (Center) and EDX (Right) Images of Irradiated NBG-18 at 13,000x. All images show the presence of nitrogen clusters along graphite plane edges.

Nitrogen clusters were not observed on the surface of irradiated NBG-25, though results from EDX indicated a substantial nitrogen presence (~10 at. %). Using a focused ion beam (FIB), a cross section of material was removed from the surface of one of the irradiated NBG-25 samples in order to investigate any possible source of sub-surface nitrogen; the area of material removed measured approximately 25 □m (length □m (depth). At a depth of ~1 □m, cluste within a closed pore that was exposed by the removal of material using the FIB (Fig. 5). As was observed for irradiated POCOFoam and NBG-18, the nitrogen clusters have bonded preferentially along edges within the pore.

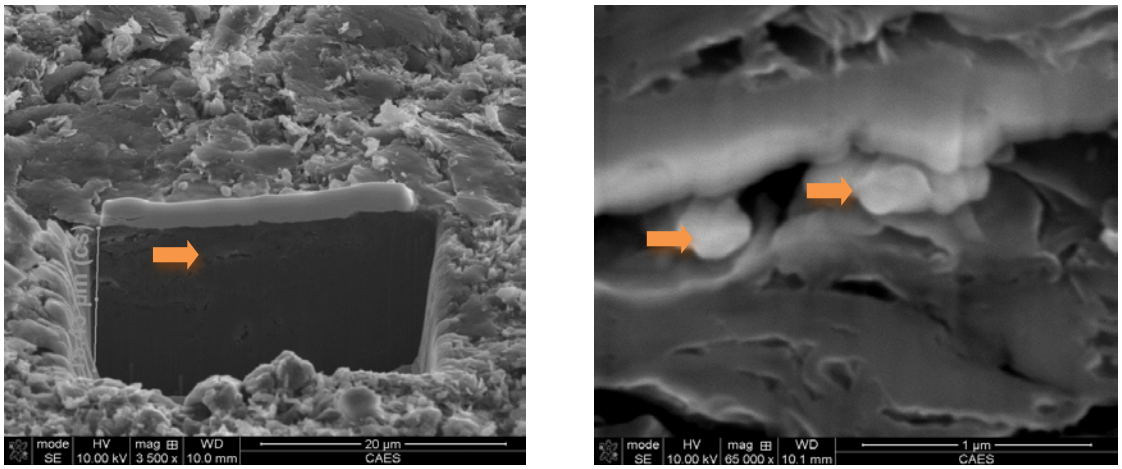

Fig. 5. SEM Images of Irradiated NBG-25 at 3500x (left) and 65000x (right). Nitrogen clusters (indicated by arrows, right image) are observed within a previously closed pore (arrow, left image).

The chemical environment of the graphite surface was investigated using XPS and SIMS.

Analysis of XPS results did not reveal measurable concentrations of nitrogen on the surface of the unirradiated non-LN immersed NBG-18 or POCOFoam samples, or unirradiated NBG-25 samples. Results from the XPS spectra of the unirradiated LN-immersed samples showed measurable concentrations of nitrogen on the surface; concentration levels varied from 0.01-0.67 atom% in POCOFoam, and 0.34-0.42 atom% in NBG-18. Surfaces of the irradiated POCOFoam and NBG-18 samples contained much larger nitrogen concentrations (36.1 atom% and 38.7 atom%, respectively) than the unirradiated samples; surfaces of the irradiated NBG-25 contained no significant

quantities of nitrogen (0.22 atom%). The amount of surface nitrogen regressed to insignificant values (less than 1.0 atom %) for all post-thermal treatment graphites.

The most significant non-nitrogen species found on the surfaces of all graphite samples was oxygen, ranging from 1.0-1.3 atom% for unirradiated POCOFoam and NBG-18, and 2.8 atom% for unirradiated NBG-25. Those values increased to 25.2 atom%, 17.3 atom%, and 6.8 atom%, respectively, for the irradiated cases. Oxygen values for all thermally treated irradiated graphite samples were also reduced (approximately 2.0 atom% for POCOFoam and NBG-18 samples, and 6.0 atom% for NBG-25), but were still larger than for unirradiated samples.

A side-by-side comparison of the unirradiated, unirradiated LN-immersed, irradiated, and thermally treated irradiated cases for each graphite type is shown in Figure 6; note that samples of NBG-25 were LN-immersed for the purpose of comparison with the other graphite types, but were not irradiated.

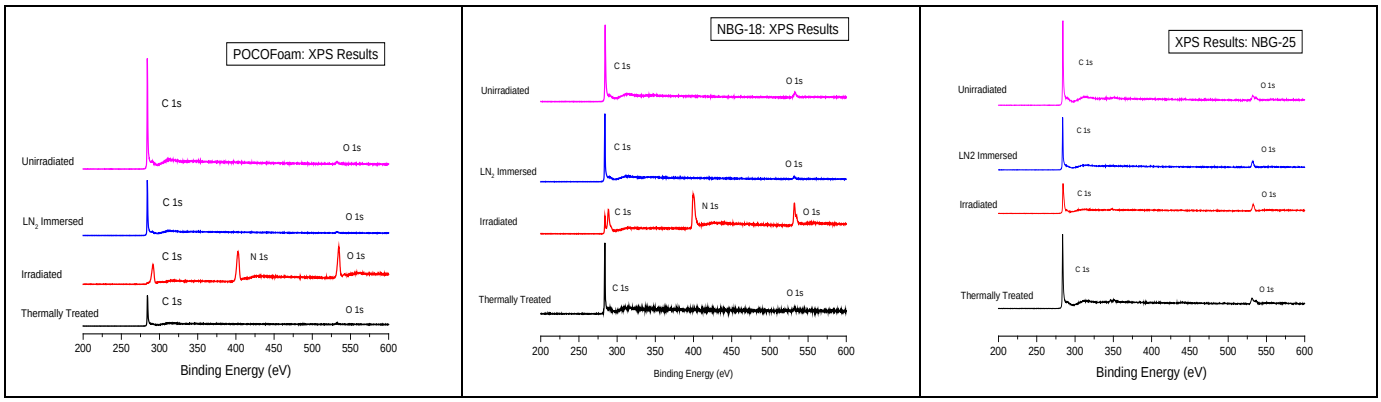

Fig. 6. XPS Survey Scans for Unirradiated/LN_2-Immersed/Irradiated/Thermally Treated Irradiated Samples of POCOFoam (left), NBG-18 (center), and NBG-25 (right)

The chemical environment at the surface was investigated for all graphite types. Deconvolution of the XPS C 1s and N 1s peaks for the irradiated graphites allowed the bonding types between the carbon, oxygen, and nitrogen atoms to be evaluated. The results for the identification of bond types on the surface of each irradiated graphite type (discussed in [15]) are summarized in Figure 7 and Table V.

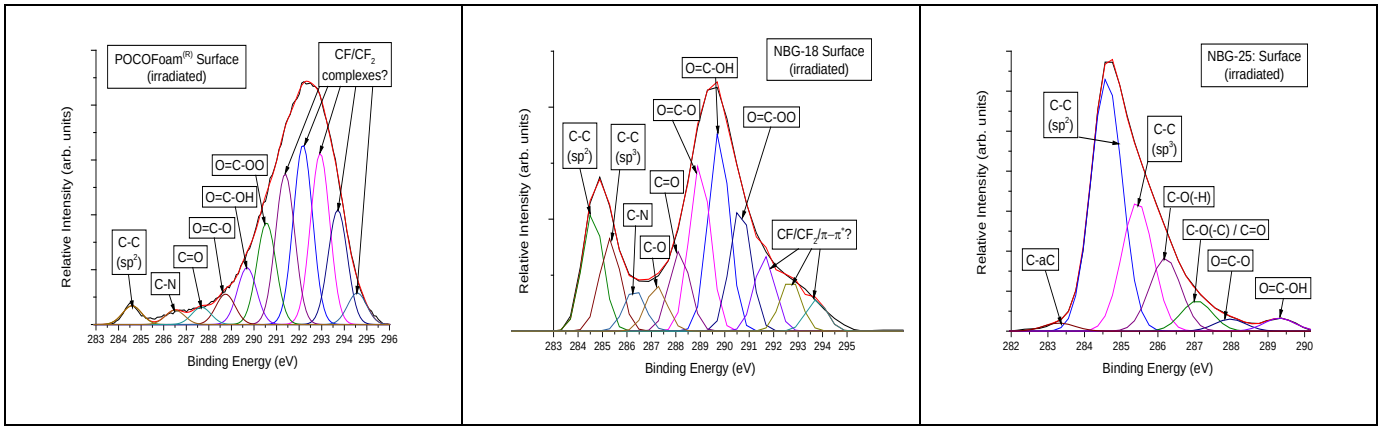

Fig. 7. XPS C 1s Peaks for Irradiated POCOFoam (left), NBG-18 (center), and NBG-25 (right)

Table V. Summary of Surface Bonds Present for All Irradiated Graphite Types, via XPS

Bond Type	Irradiated POCOFoam	Irradiated NBG-18	Irradiated NBG-25
C-C (sp^2)	2.1	11.6	48.7
C-C (sp^3)	0.0	9.0	24.9
C-N	1.6	4.1	0.0
C-O-(H, C)	0.0	4.4	14.1
C=O	1.9	7.8	5.8
O=C-O	3.4	16.3	2.3
O=C-O-(O, H)	17.9	31.5	2.5

Only a small portion of the total surface contents are contributed to nitrogen-bearing bonds for POCOFoam, which is in contrast to the information surmised from the surface scans for each graphite type (greater than 30 atom% nitrogen). The most prominent (non-carbon-carbon) surface groups are attributed to oxides: ~24% for irradiated POCOFoam, ~60% for irradiated NBG-18, and ~25% for irradiated NBG-25.

Investigation of bond type count was performed at multiple depths for each graphite type. Results of sub-surface bond population for irradiated POCOFoam and NBG-18 was presented in the WM 2013 publication [15]; a summary of bond population for NBG-25 (unirradiated vs. irradiated) is presented in Table VI.

Table VI. Summary of Bond Population for Unirradiated and Irradiated NBG-25, Surface and Sub-Sub-Surface

	Unirradiated NBG-25			Irradiated NBG-25		
Bond Type	**surface**	**3 nm**	**8 nm**	**surface**	**3 nm**	**8 nm**
C-C (sp^2)	67.8	39.4	35.9	48.7	34.4	42.7
C-C (sp^3)	19.0	25.9	28.8	24.9	30.2	28.6
C-N/C-O	0	15.2	16.6	0	0	0
C-O-H	6.8	0	0	14.1	22.0	11.9
C-O-C	0	6.4	7.3	0	7.1	0
C=O	3.4	3.7	3.6	5.8	0	4.1
O=C-O	0	0	0	2.3	2.4	1.9
O=C-OH	1.5	2.0	2.3	2.5	1.3	1.1
O=C-OO	0	1.1	1.2	0	0	0

Analysis indicates a larger concentration of carbonyl (C=O) bonding on the surfaces of irradiated graphite than that seen on the unirradiated material. The detection of carboxyl esters (O=C-O) solely in irradiated samples suggests that secondary bonding (oxygen bonding to carbon of newly formed carbonyl bonds) occurs as a direct result of neutron irradiation. The presence of hydroxyl bonds (C-OH) is minimal in unirradiated material, but is significantly increased in irradiated samples. The increase in the amount of these bonds being formed is attributed to neutron irradiation.

SIMS results indicated the presence of a limited number of nitrogen-containing species for graphites that were irradiated after LN immersion, corresponding well with XPS results. The most notable and definitive evidence that nitrogen plays some part in bonding to the surface of the graphite after irradiation is the appearance of likely cyano groups that were also seen with XPS results. The most notable species are associated with m/z value 26 in all three graphite types, and m/z values 28 and 42 in NBG-18 and POCOFoam. Continued analysis of the surface found multiple cyano molecular fragments in the mass range of 12-50 amu that confirmed the bonding of nitrogen to the surface of each of the graphites (Tables VII and VIII).

Table VII. SIMS Positive Ion Spectral Comparison of Select ^{14}C-Bearing Species, Irradiated Graphite Surfaces: Intensities Relative to ^{12}C

m/z	POCOFoam	NBG-18	NBG-25	Possible Species
14	0.046	0.035	0.488	N, ^{14}C
15	0.082	0.035	0.088	NH, ^{14}CH
16	0.318	0.097	0.024	NH_2, $^{14}CH_2$
26	0.0	0.0	0.0	CN, ^{14}CC
28	0.0	0.0	0.024	N_2, ^{14}CN
	1.425	0.614	0.0	CNH_2, $^{14}CCH_2$
29	0.0	0.0	0.137	N_2H, ^{14}CNH
30	0.208	0.056	0.017	NO, ^{14}CO
	0.0	0.0	0.020	N_2H_2, $^{14}CNH_2$
42	0.0	0.001	0.024	CNO, ^{14}C-O-C
	0.0	0.0	0.044	N_3, ^{14}C-^{14}C-^{14}C
46	0.0	0.001	0.0	NO_2, $^{14}CO_2$

Table VIII. SIMS Negative Ion Spectral Comparison of Select ^{14}C-Bearing Species, Irradiated Graphite Surfaces: Intensities Relative to ^{12}C

m/z	POCOFoam	NBG-18	NBG-25	Possible Species
14	0.0	0.0	0.049	N, ^{14}C
15	0.132	0.126	0.011	NH, ^{14}CH
16	0.0	0.0	0.0	NH_2, $^{14}CH_2$
26	4.093	9.905	0.144	CN, ^{14}CC
28	0.003	0.007	0.0	N_2, ^{14}CN
	0.0	0.0	0.0	CNH_2, $^{14}CCH_2$
29	0.0	0.0	0.0	N_2H, ^{14}CNH
30	0.048	0.050	0.001	NO, ^{14}CO
	0.0	0.001	0.0	N_2H_2, $^{14}CNH_2$
42	1.654	1.286	0.0	CNO, ^{14}C-O-C
	0.0	0.0	0.0	N_3, ^{14}C-^{14}C-^{14}C
46	0.003	0.004	0.0	NO_2, $^{14}CO_2$

It is possible that the ion signature at ~14 amu for irradiated POCOFoam and NBG-18 may be activated C-14 atoms or a singly ionized nitrogen atom; however, as discussed above it is difficult to distinguish between the masses of the two atoms. The EDX results show significant nitrogen presence on the surface, and the XPS results indicate high nitrogen concentrations. Thus, it was assumed that singly ionized nitrogen atoms contribute a majority of the 14 amu peak.

The ~14 amu ion signature for irradiated NBG-25 is more likely to indicate the presence of C-14 based on the relative lack of nitrogen presence on the surface, as determined by the results from XPS and SEM/EDX. This principle is reinforced when considering the nature of the 26 amu (negative ion) peak, which would seem to indicate a substantial presence of nitrogen atoms in CN- ion fragments. Given the absence of any significant presence of nitrogen using other analysis techniques, it is proposed that even bound 'nitrogen' atoms (i.e. atoms that indicate nitrogen via their mass) are in fact bound C-14 atoms. This is also likely for ion signatures that might incorporate nitrogen atoms as a part of the released ion fragment, such as 42 amu (^{14}C-O-C instead of CNO), which is attributed to ^{14}C-bearing surface ether groups. This reasoning cannot be applied to the 26 amu signal for irradiated POCOFoam or NBG-18, given the significant presence of nitrogen detected by both XPS surface scans and EDX; therefore, it cannot be determined with any precision whether any presence of 'nitrogen' atoms are indeed N-14, or C-14.

SIMS was also used to investigate the surface dependency of specific species in irradiated graphite. A summary of the amount remaining of a particular species at a depth of ~5 nm (when compared to surface amounts) is provided in Table IX (positive ion spectra) and Table X (negative ion spectra).

Table IX. SIMS Positive Ion Spectral Comparison of Surface and Sub-Surface Species, All Irradiated Graphite Types (N/A indicates that no initial surface content was present)

m/z	Amount Remaining Post-Sputter, 5 nm (%)			Possible Species
	POCOFoam	NBG-18	NBG-25	
14	0.0	23.3	11.6	N, ^{14}C
15	0.0	8.0	34.0	NH, ^{14}CH
16	34.6	11.7	0.0	NH_2, $^{14}CH_2$
26	N/A	N/A	N/A	CN, ^{14}CC
28	N/A 52.1	N/A 14.3	79.0 N/A	N_2, ^{14}CN CNH_2, $^{14}CCH_2$
29	N/A	N/A	113.3	N_2H, ^{14}CNH
30	0.0 N/A	11.7 N/A	0.0 0.0	NO, ^{14}CO N_2H_2, $^{14}CNH_2$
42	N/A N/A	~1800 N/A	94.8 0.0	CNO, ^{14}C-O-C N_3, ^{14}C-^{14}C-^{14}C
46	N/A	0.0	N/A	NO_2, $^{14}CO_2$

Table X. SIMS Negative Ion Spectral Comparison of Surface and Sub-Surface Species, All Irradiated Graphite Types

m/z	Amount Remaining Post-Sputter, 5 nm (%)			Possible Species
	POCOFoam	NBG-18	NBG-25	
14	N/A	N/A	8.6	N, ^{14}C
15	13.4	3.2	0.0	NH, ^{14}CH
16	N/A	N/A	N/A	NH_2, $^{14}CH_2$
26	581.0	245.4	265.9	CN, ^{14}CC
28	1009.0 N/A	248.0 N/A	N/A N/A	N_2, ^{14}CN CNH_2, $^{14}CCH_2$
29	N/A	N/A	N/A	N_2H, ^{14}CNH
30	38.4 N/A	13.4 23.7	0.0 N/A	NO, ^{14}CO N_2H_2, $^{14}CNH_2$
42	105.7 N/A	30.7 N/A	N/A N/A	CNO, ^{14}C-O-C N_3, ^{14}C-^{14}C-^{14}C
46	183.3	166.0	N/A	NO_2, $^{14}CO_2$

The ion signatures for 26 amu (CN or ^{14}CC) in the negative ion spectrum and 42 amu (CNO or ^{14}C-O-C) in the positive ion spectrum indicate that a significant portion of possible C-14 contamination persists at shallow depths below the graphite surface. These species are attributed to nitrogen that diffused into the sample prior to, or during, the early stages of irradiation, as graphite lattice bonds were severed by neutron bombardment; nitrogen then formed bonds within the lattice, and was thereafter transmuted to C-14. In most other cases, the lack of substantial presence of 14 amu-bearing atoms at a depth of 5 nm indicates that a significant portion of C-14 contamination is concentrated within the first few layers of the surface.

Thermally treated irradiated graphite

The process of thermal treatment severely degraded the surfaces of each irradiated graphite type, as shown using SEM (Fig. 8). The resulting surface was uneven and much more porous than pre-treated surfaces.

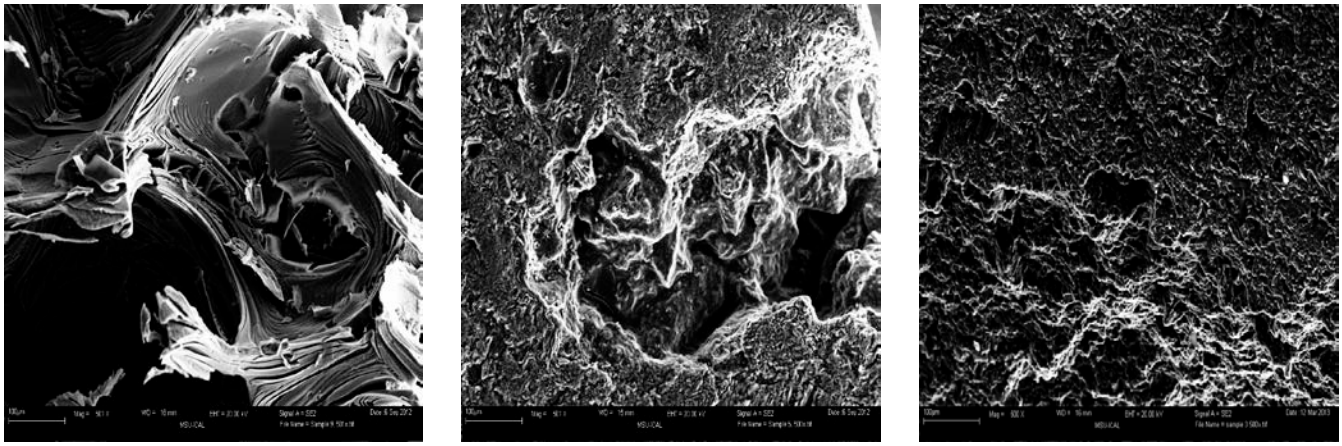

Fig. 8. SEM Images of Thermally Treated Irradiated POCOFoam (Left), NBG-18 (Center) and NBG-25 (Right) at 500x.

Based on the results of off-gas analysis from the thermal treatment process and the previously reported XPS surface scan for each irradiated graphite type, it was expected that a significant portion of surface oxides that were present on irradiated graphites would not exist on the surfaces of thermally treated irradiated graphites. Deconvolution of the C 1s peak for each thermally treated graphite type confirms this expectation (Fig. 9).

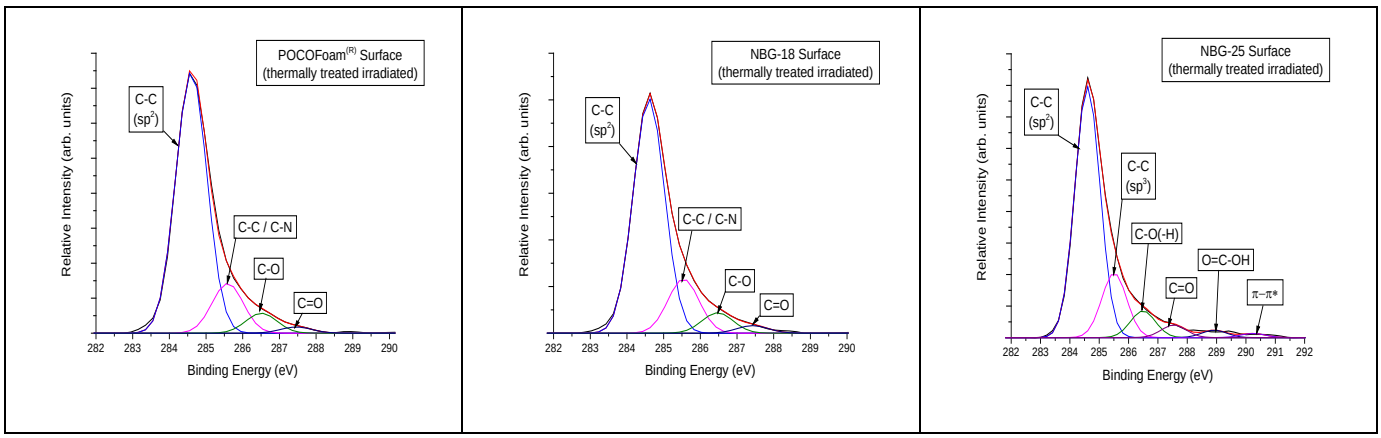

Fig. 9. XPS C1s Peaks for Thermally Treated Irradiated POCOFoam (left), NBG-18 (center), NBG-25 (right).

The extent of peak broadening that was observed for irradiated graphite samples is reduced in thermally treated irradiated graphite samples. Both the types and amounts of surface oxides present in thermally treated irradiated graphite samples is significantly less when compared to irradiated samples. A summary of individual bond types for the surface of each thermally treated irradiated graphite type is provided in Table XI.

Table XI. Summary of Surface Bonds Present for All Thermally Treated Irradiated Graphite Types, via XPS

Bond Type	**Thermally Treated Irradiated POCOFoam**	**Thermally Treated Irradiated NBG-18**	**Thermally Treated Irradiated NBG-25**
C-C (sp^2)	77.5	72.9	68.5
C-C (sp^3)/C-N	14.8	16.9	17.6
C-O-(C,H)	5.9	7.7	7.3
C=O	1.8	2.5	3.4
O=C-O	0.0	0.0	0.0
O=C-O-(O,H)	0.0	0.0	2.0

The presence of carboxyl esters (O=C-O) are non-existent in thermally treated irradiated graphite samples, and the amount of carbonyl (C=O) groups is significantly less when compared to pre-thermal treatment irradiated samples. An overall regression in the amount of other surface oxide groups (hydroxyls, ethers, carbonates) is also observed (Table XII.)

Table XII. XPS Comparison of Carbon Bonds for Unirradiated, Irradiated, and Thermally Treated Irradiated NBG-25

	Unirradiated NBG-25			**Irradiated NBG-25**			**Thermally Treated Irradiated NBG-25**		
Bond Type	**surface**	**3 nm**	**8 nm**	**surface**	**3 nm**	**8 nm**	**Surface**	**3 nm**	**8 nm**
C-C (sp^2)	67.8	39.4	35.9	48.7	34.4	42.7	68.5	52.0	46.1
C-C (sp^3)	19.0	25.9	28.8	24.9	30.2	28.6	17.6	23.1	23.8
C-N/C-O	0	15.2	16.6	0	0	0	0	0	0
C-O-H	6.8	0	0	14.1	22.0	11.9	7.3	10.2	11.8
C-O-C	0	6.4	7.3	0	7.1	0	0	0	0
C=O	3.4	3.7	3.6	5.8	0	4.1	3.4	5.1	5.7
O=C-O	0	0	0	2.3	2.4	1.9	0	0	3.4
O=C-OH	1.5	2.0	2.3	2.5	1.3	1.1	2.0	2.5	2.0
O=C-OO	0	1.1	1.2	0	0	0	0	1.4	0
C-aC	1.4	6.3	4.3	1.6	2.6	9.7	0	5.6	5.7
□□□ *	0	0	0	0	0	0	1.1	1.4	1.4

Lesser quantities of hydroxyl groups are detected in post-thermal treatment, irradiated material, but still in greater amounts than in pre-irradiated material. A general regressive trend in the amounts of carbon-oxygen functional groups (carbonyls, esters) present in thermally treated, irradiated graphite, when compared to pre-treated irradiated graphite, is observed.

Results for SIMS analysis (positive ion spectrum) of thermally treated irradiated graphite confirm the findings from XPS for specific ion compounds and fragments (Table XIII).

Table XIII. SIMS Positive Ion Spectral Comparison of Select ^{14}C-Bearing Species, Thermally Treated Irradiated Surfaces: Intensities Relative to ^{12}C

m/z	**POCOFoam**	**NBG-18**	**NBG-25**	**Possible Species**
14	0.400	1.466	0.174	N, ^{14}C
15	0.0	0.0	1.504	NH, ^{14}CH
16	0.0	0.030	0.0	NH_2, $^{14}CH_2$
26	0.0	0.0	1.193	CN, ^{14}CC
28	0.0	0.0	0.486	N_2, ^{14}CN
	0.0	1.980	0.798	CNH_2, $^{14}CCH_2$
29	0.0	0.0	0.0	N_2H, ^{14}CNH
30	0.0	0.025	0.0	NO, ^{14}CO
	0.0	0.049	0.0	N_2H_2, $^{14}CNH_2$
42	0.0	0.064	0.055	CNO, ^{14}C-O-C
	0.0	0.093	0.156	N_3, ^{14}C-^{14}C-^{14}C
46	0.0	0.0	0.0	NO_2, $^{14}CO_2$

The presence of 14 amu in thermally treated irradiated POCOFoam and NBG-18 samples was expected based on the saturated nitrogen environment under which irradiation of those samples took place. Significant amounts of several ^{14}C-bearing species are detected in thermally treated samples of NBG-25, which was somewhat unexpected; the cause of this phenomenon is being investigated through further thermal treatment studies.

Thermal Treatment

Thermal treatment off-gas speciation was measured during the experiments by the inline gas analyzer. Fig. 10 shows corrected gas analyzer data representative of the unirradiated and irradiated NBG-18 experiments at 700°C. (POCOFoam gasification was detailed in the previous paper, while the nuclear grade graphite will be highlighted here.) CO and CO_2 were the major species released from the graphite. It appears that when NBG-18 oxidation is limited to use of previously adsorbed oxygen species (no oxygen in carrier gas) the removal of carbon is highly limited. The main desorption pathway during the gasification of both unirradiated and irradiated NBG-18 at 700°C and Ar + 5vol% O_2 is CO. Further the desorption rate appears to decrease with respect to time at temperature. The low porosity and low impurity concentration of this graphite likely means fewer active sites available for oxygen adsorption and subsequent oxidation. The initial increase in the release of carbon from the NBG-18 at temperature is likely a result of the oxidation of the most chemically active environments on the graphite.

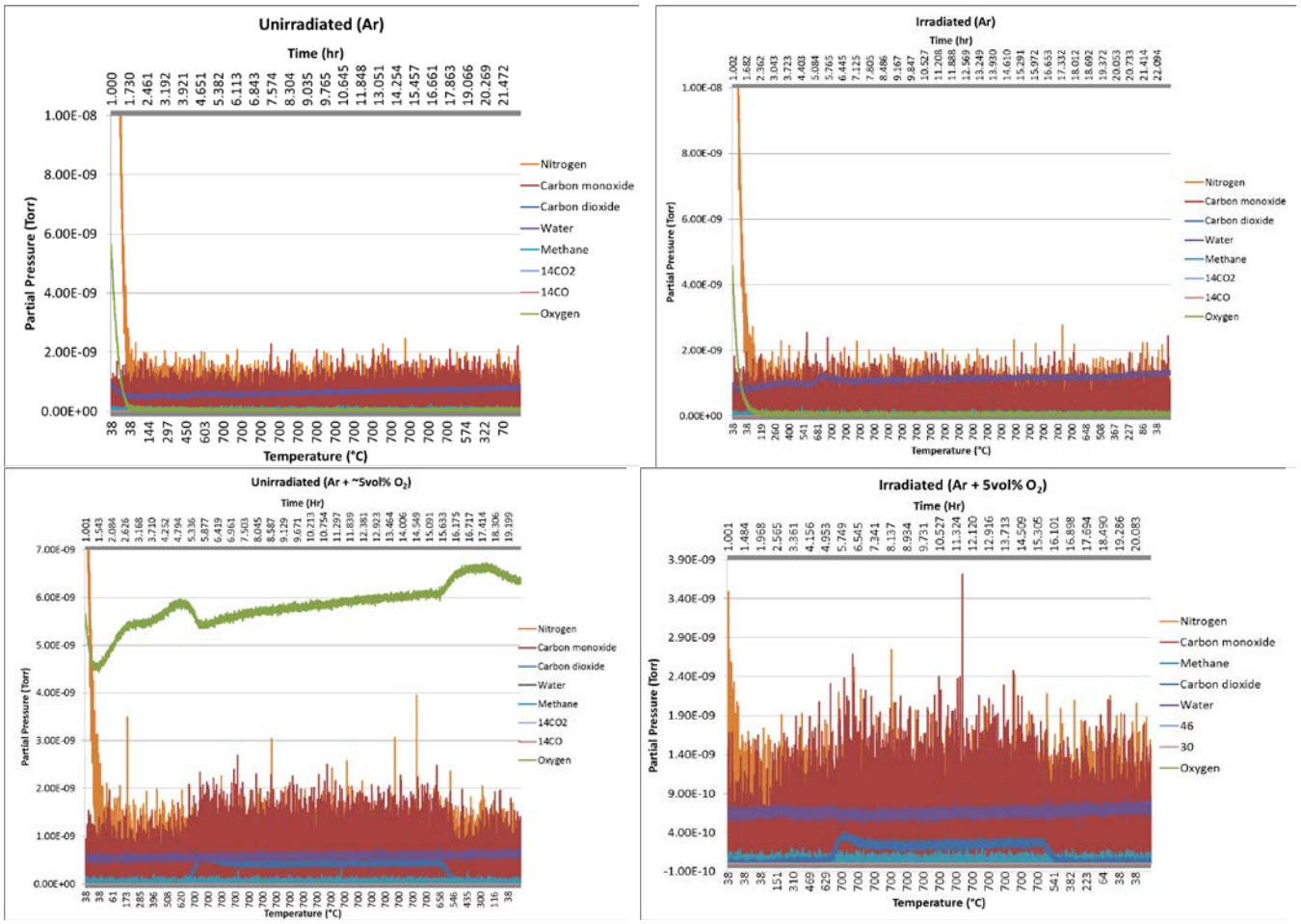

Fig. 10. Off-gas Speciation during Gasification of NBG-18 at 700°C

At 1400°C there is a shape different from the off-gas species curves at 700°C (see Fig. 11.) During heating (to 1400°C), the graphite oxidation kinetics is first dominated by chemical rate of reaction, then by reactant and product diffusion in the graphite (between approximately 800°C and 1200°C) and by boundary layer diffusion at the higher temperatures. Gasification occurring within the diffusion controlled kinetic regime follows the same trends seen during the oxidation of graphite at 700°C.

At 1400°C the release rate appears to increase with respect to time. The increase likely indicates that as additional C-C bonds are broken there is an increase in active sites available for oxidation. As seen during the gasification of NBG-18 at 700°C, CO is the primary desorption species during the diffusion controlled kinetic regime and CO is even more dominant during the boundary layer controlled regime.

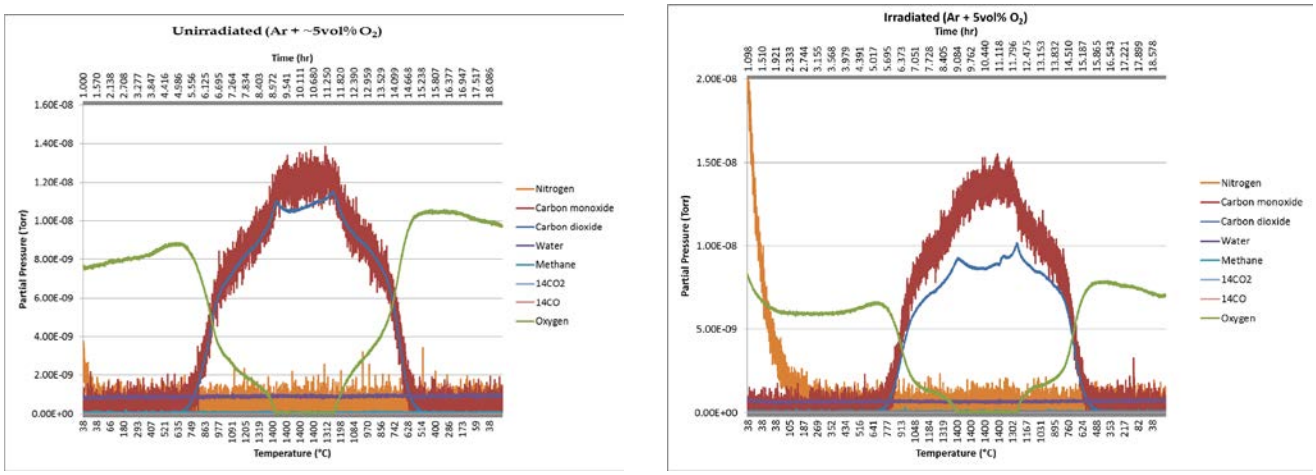

Fig. 11. Off-gas Speciation during Gasification of NBG-18 at 1400°C

Though there is limited evidence of oxidation of NBG-18 at 700°C, results of C-14 analysis indicate its efficient removal under these conditions. To evaluate thoroughly the selective release of ^{14}C over ^{12}C, release data (obtained via liquid scintillation counting off gas collection solution) were normalized for each sample's mass, activity, and the experimental time and then averaged over the number of samples tested. The results of these calculations are presented in Table XIV. Larger values denote more selective release of C-14.

Table XIV. Relative Release of Carbon-14 during Thermal Treatment of Irradiated Graphites

Normalized Averaged Relative Percentage Release Ratio C-14:C-12					
700°C		**900°C**		**1400°C**	
POCOFoam	**NBG-18**	**POCOFoam**	**NBG-18**	**POCOFoam**	**NBG-18**
	(0 vol% O_2) 195.49	(0 vol% O_2) 42.14		(0 vol% O_2) 38.49	
(3 vol% O_2) 8.08				(3 vol% O_2) 2.85	
(5 vol% O_2) 5.89	(5 vol% O_2) 11.17			(5 vol% O_2) 1.57	(5 vol% O_2) 2.55

The values in Table XIV suggest that the oxygen level has the greatest influence on the selective release rate followed by temperature. Lower oxygen levels and lower temperatures within each oxygen level studied provide the most selective release of ^{14}C.

DISCUSSION

Characterization

Previously reported results from structural characterization techniques indicated significant radiation damage and the formation of an amorphous phase on the graphite surface. These results indicate an increase in disorder and disorientation of the carbon atoms in the graphite lattice structure. Disruption to the graphite lattice can provide multiple bonding sites where nitrogen can become chemically bound both to the surface and within the structure. The existence of micron-sized opaque nitrogen clusters, observed using SEM and EDX, along the planar edges of

LN-immersed irradiated graphite samples supports this principle. Results of XPS analyses of post-irradiated samples indicate increased quantities of carbon-nitrogen (POCOFoam and NBG-18) and carbon-oxygen (all graphite types) bonds are directly correlated to broken bonds in the graphite lattice caused by sample irradiation.

Chemical analysis mapped variations in the spatial chemical composition of the graphite surface after irradiation. XPS results confirmed increased concentrations of nitrogen on the surface of LN-immersed graphite samples after irradiation. Measurable concentrations of the nitrogen atoms and corresponding bonding types were seen up to a minimum depth of 100 nm, indicating that the nitrogen atoms are chemically bound within the graphite structure. The discovery of bound nitrogen clusters deep within irradiated NBG-25 samples indicates that neutron irradiation causes lattice disruptions far beneath the surface layers of the graphite. The concentrations of the carbon-nitrogen and carbon-oxygen species decrease deeper into the graphite, observed through sputtering below the surface.

The observation of various nitrogen-bearing species, particularly for m/z values 26 and 42, in SIMS results indicates the substitution of single nitrogen atoms into displaced carbon atom locations in the graphite lattice. It is interesting to note that the relative concentrations of most nitrogen-containing species present on the surface of irradiated NBG-25 are greater than those for the irradiated LN-immersed graphites. The confirmation of single and diatomic nitrogen atoms substituted into the carbon rings despite irradiation dictates that C-14 could also be found at these locations. Furthermore, the presence of strongly bonded carbon-nitrogen atoms deep within the graphite structure also indicates C-14 could be found at similar locations. SIMS results revealed that N_2 drastically decreases within the first 10 nm of depth, indicating that it likely exists as a weakly bonded sub-layer on the surface of the graphite. Therefore, any C-14 produced as a result of the activation of the weak N_2 sub-layer should be readily removed by thermal treatment. This removal may be evidenced by the high initial C-14 release rates seen during the first hour of thermal treatment. At all experimental temperatures, a large amount of C-14 was immediately released; the C-14 release rate then decreased before again increasing.

It is important to note that the results of previously reported XRD, Raman, SIMS, and XPS analyses indicate that LN immersion does not induce a measureable change in the graphite structure prior to irradiation, while the results presented here confirm an increased nitrogen presence in post-irradiated samples.

Thermal Treatment

Both CO_2 and CO were released during thermal treatment of NBG-18, but the dominant off gas species at all thermal treatment temperatures was CO. However, the relative amount of CO to CO_2 increases with addition of oxygen at the lower temperature. The ratio CO:CO_2 also increases with temperature increase, which pushes the oxidation kinetics regime from diffusion controlled to boundary layer controlled. These results are consistent with XPS results indicating specific surface bonded carbon-oxygen functional groups that release CO_2 at lower temperatures and CO at higher temperatures. Aldehydes, carboxylics and lactones release CO_2 from 150-650°C, with limited desorption at higher temperatures. Ethers, ketones and quinones release CO starting at 700°C.

Selective release of C-14 is positively influenced by low oxygen level and low treatment temperature. Indeed, the most efficient C-14 removal in the experiments occurred with NBG-18 heated to 700°C in argon gas with no oxygen added. Oxidation in this instance occurred via species on the irradiated graphite surfaces. Based on these results, new experiments have been designed to pre-load the irradiated graphite surfaces with oxygen before heating to the thermal treatment temperatures in an argon atmosphere.

SUMMARY AND CONCLUSIONS

Among other routes, carbon-14 found in irradiated graphite is created through neutron activation of N-14. Understanding the location, bonding configuration, and chemical environment of N-14 has led to a greater understanding of the locations, bonding configurations, and chemical environments in which C-14 is present in irradiated graphite. Irradiated graphite thermal treatment to remove C-14 offers additional insight to its chemical

nature. A greater understanding of the chemical and physical environments of C-14 is helping to optimize its removal as a waste management technique.

Characterization of irradiated graphite surfaces revealed strongly bound nitrogen clusters on the surfaces of irradiated POCOFoam and NBG-18 graphites, which were immersed in liquid nitrogen prior to irradiation. Similar clusters were not found on the surface of NBG-25, which was irradiated in the presence of flowing He, but clusters were observed within exposed closed pores located approximately 1 [illegible] beneath the surface.

XPS analysis revealed that the most notable differences between the pre- and post-irradiated graphites are in the types of C-C, C-N, and C-O bonding. Further, results of SIMS analysis indicate various combinations of functional groups dominating according to graphite type. Each irradiated graphite has high concentrations of functional groups at 26 and 42 amu, with likely formulas being CN, ^{14}CC, CNO, ^{14}C-O-C. Furthermore, both graphites that were irradiated in nitrogen-rich environments has a significant proportion of functional groups with masses 28 amu (N_2, ^{14}CN) while NBG-25 has a relatively high concentration functional groups relating to 14 amu (with possible formulas N and ^{14}C, though the relative lack of nitrogen detected via other techniques suggests that this signature is prominently C-14).

The concentrations of certain carbon-containing functional groups are location-specific: carboxylates are most prominent on graphite surfaces, while ether groups reside deeper within the sample – the location of specific ^{14}C-bearing functional groups could be used to specifically target the desorption of ^{14}C-bearing gaseous products (CO vs. CO_2). Significant amounts of sub-surface C-14 bound within the irradiated graphite (detected as ^{14}C-C species) were also observed.

Thermal treatment experiments indicate that selective release of C-14 is greatest at the lowest oxidant level and temperature. Removing a majority of the most significant long-lived radionuclide would reduce the volume of radioactive waste needing to be sent to a deep geological repository and allow the remaining nuclear grade graphite to be recycled.

Future work includes pre-loading of oxygen to irradiated graphite surfaces prior to heating to thermal treatment temperatures under flowing inert gas.

REFERENCES

1. FACHINGER, J., PODRUHZINA, T., VON LENSA, W., "*Decontamination of Nuclear Graphite by Thermal Treatment*," Solutions for Graphite Waste, Manchester, UK (March 2007).
2. IDAHO NATIONAL LABORATORY, "*Next Generation of Reactors.*" https://inlportal.inl.gov/portal/server.pt?open=514&objID=1361&parentname=CommunityPage&parentid=9&mode=2
3. GEN-IV INTERNATIONAL FORUM, "*The Very-High-Temperature Reactor (VHTR) is a graphite-moderated, helium-cooled reactor with a thermal neutron spectrum.*" http://www.gen-4.org/Technology/systems/vhtr.htm
4. NUCLEAR ENERGY AGENCY, "*Generation IV International Forum*," Technical Secretariat, 2009.
5. PODRUHZINA, TATJANA, "*Graphite as radioactive waste: corrosion behavior under final repository conditions and thermal treatment,*" Doctoral Dissertation, 2004.
6. LaBrier, Daniel P., "Characterization of ^{14}C in Neutron-Irradiated Graphite," PhD Dissertation in Nuclear Engineering, Idaho State University, 2013.
7. McCrory, Shilo M., "Characterizing the Pathway to Formation of ^{14}C in Irradiated Graphite," MS Thesis in Nuclear Science and Engineering, Idaho State University, 2011.
8. ELECTRIC POWER RESEARCH INSTITUTE, "*Graphite Decommissioning: Options for Graphite Treatment, Recycling, or Disposal, including a Discussion of Safety-Related Issues,*" EPRI Technical Report 1013091(March 2006).

9. Smith, Tara E., McCrory, Shilo, Dunzik-Gougar, M.L., "Limited Oxidation of Irradiated Graphite Waste to Remove Surface Carbon-14", Journal of Nuclear Engineering and Technology (JoNET), Vol. 3, No. 1 (2013)
10. Briggs, D., Seah, M.P., *"Practical Surface Analysis by Auger and X-ray Photoelectron Spectroscopy,"* John Wiley and Sons, 1983.
11. Yates, J.T. Jr., Madey, T., Erickson, N., *"ESCA Study of Carbon Monoxide and Oxygen Adsorption on Tungsten."* XPS PhotoElectron Spectroscopy, Benchmark Papers in Physical Chemistry and Chemical physics V.2. 1978.
12. IAEA, *"The Thermal Oxidation of Graphite,"* Irradiation Damage in Graphite due to Fast Neutrons in Fission and Fusion Systems, IAEA-TECDOC-1154, April 2000.
13. POCO Graphite, INC. http://www.POCOFoam.com/tabid/130/Default.aspx
14. Cleaver, J., McCrory, S., Smith, T., and Dunzik-Gougar, M.L., "Chemical Characterization and Removal of Carbon-14 from Irradiated Graphite," WMS 2012, Phoenix, February 2012.
15. Dunzik-Gougar, M.L., Cleaver, J., McCrory, S. and Smith, T., "Chemical Characterization and Removal of Carbon-14 from Irradiated Graphite II," WMS 2013, Phoenix, February 2013.

ACKNOWLEDGEMENTS

This research was partially performed using funding received from the DOE Office of Nuclear Energy's Nuclear Energy University Programs.